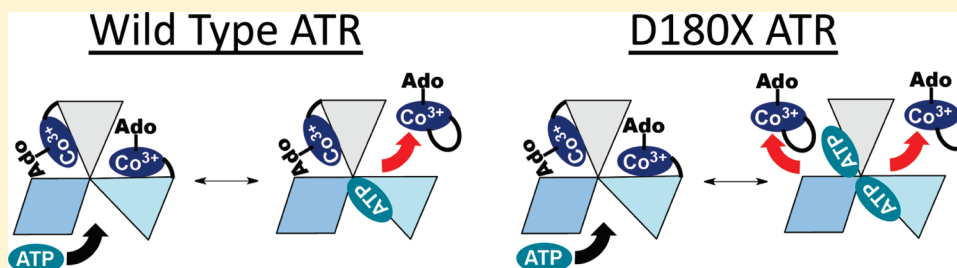


Loss of Allostery and Coenzyme B₁₂ Delivery by a Pathogenic Mutation in Adenosyltransferase

Michael Lofgren and Ruma Banerjee*

Department of Biological Chemistry, University of Michigan Medical Center, Ann Arbor, Michigan 48109-0600, United States

ABSTRACT:



ATP-dependent cob(I)alamin adenosyltransferase (ATR) is a bifunctional protein: an enzyme that catalyzes the adenosylation of cob(I)alamin and an escort that delivers the product, adenosylcobalamin (AdoCbl or coenzyme B₁₂), to methylmalonyl-CoA mutase (MCM), resulting in holoenzyme formation. Failure to assemble holo-MCM leads to methylmalonic aciduria. We have previously demonstrated that only 2 equiv of AdoCbl bind per homotrimer of ATR and that binding of ATP to the vacant active site triggers ejection of 1 equiv of AdoCbl from an adjacent site. In this study, we have mimicked in the *Methylobacterium extorquens* ATR, a C-terminal truncation mutation, D180X, described in a patient with methylmalonic aciduria, and characterized the associated biochemical penalties. We demonstrate that while k_{cat} and $K_{\text{M}}^{\text{Cob(I)}}$ for D180X ATR are only modestly decreased (by 3- and 2-fold, respectively), affinity for the product, AdoCbl, is significantly diminished (400-fold), and the negative cooperativity associated with its binding is lost. We also demonstrate that the D180X mutation corrupts ATP-dependent cofactor ejection, which leads to transfer of AdoCbl from wild-type ATR to MCM. These results suggest that the pathogenicity of the corresponding human truncation mutant results from its inability to sequester AdoCbl for direct transfer to MCM. Instead, cofactor release into solution is predicted to reduce the capacity for holo-MCM formation, leading to disease.

Coenzyme B₁₂ or 5'-deoxyadenosylcobalamin (AdoCbl) is a complex organometallic cofactor that is used in all domains of life by enzymes catalyzing diverse reactions including: dehydrations, intramolecular carbon skeleton rearrangements, reductive eliminations, and deaminations.^{1–3} AdoCbl comprises a central cobalt ion coordinated equatorially by four nitrogen atoms donated by the corrin macrocycle. A novel nucleotide base, dimethylbenzimidazole (DMB), occupies the lower axial coordination position while the upper axial position is occupied by the 5'-deoxyadenosyl group, via the organometallic cobalt–carbon bond.

AdoCbl is a “high value” product that is either biosynthesized *de novo* by some bacteria or generated via adenosylation of cob(I)alamin in organisms such as mammals, which lack a *de novo* pathway for its synthesis.⁴ There are at least three families of ATP-dependent cob(I)alamin adenosyltransferases (ATR): EutT, PduO, and CobA, which catalyze the addition of the 5'-deoxyadenosyl group from ATP to cob(I)alamin; however, their roles in metabolism are distinct. Members of the three ATR subfamilies do not share sequence or structural homology and represent examples of convergent evolution. In some organisms, such as *Salmonella enterica*, members of all three ATR subfamilies are used to meet metabolic requirements under distinct

physiological conditions.⁴ The EutT- and PduO-type ATRs of *S. enterica* furnish AdoCbl for the B₁₂-dependent enzymes, diol dehydratase, and ethanolamine ammonia lyase, for catabolism of alkane diols and growth on ethanolamine, respectively.^{2,5} In contrast, CobA is involved in the *de novo* synthesis of AdoCbl.⁶ Humans use a PduO-type ATR for supplying AdoCbl to the only enzyme that uses this cofactor, i.e. MCM, for catabolism of cholesterol, branched chain amino acids, and odd-chain fatty acids.^{7,8}

To overcome the twin challenges posed by the lability of the cofactor in the three biologically relevant cobalt oxidation states and its low tissue concentration in humans, it has been proposed that, following intracellular delivery, B₁₂ remains protein-bound as it is processed and delivered to its target enzymes.^{9,10} In support of this model, it has been demonstrated that, following AdoCbl synthesis by ATR, the cofactor is directly transferred to the active site of MCM via a transient protein–protein interaction.^{11–13} Mutations in ATR lead to deficiencies in the

Received: April 25, 2011

Revised: May 20, 2011

Published: May 23, 2011

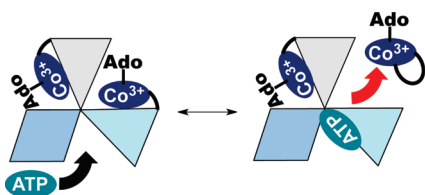


Figure 1. ATP binding triggers AdoCbl release. The ATR·product complex has two of three active sites occupied by AdoCbl. The three subunits of ATR are depicted in shades of blue and gray. ATP binds to the ATR·2AdoCbl complex and triggers the release of 1 equiv of AdoCbl. In the presence of MCM, AdoCbl is transferred directly in the “base-off” conformation.

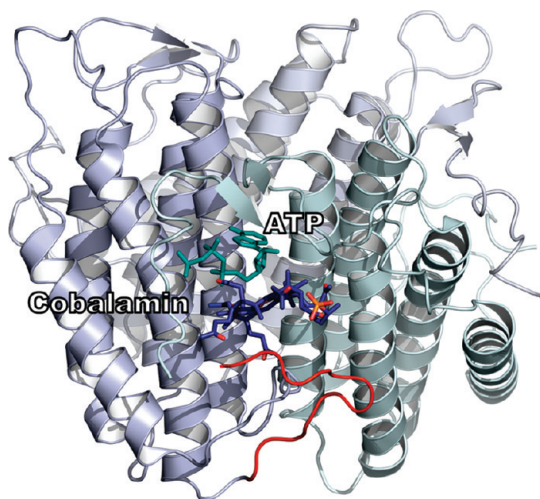
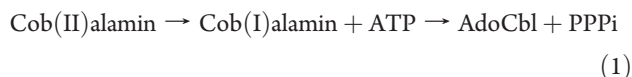


Figure 2. Structure of PduO-type ATR from *L. reuteri* with AdoCbl and ATP bound (PDB entry 3CI1). The ATR holoenzyme is shown in ribbon representation with the individual subunits of the ATR trimer colored as in Figure 1. ATP and cobalamin are shown in stick representation in cyan and dark blue, respectively. The C-terminal loop (red) in one subunit corresponds to the boundaries of the truncation in *M. extorquens* D180X ATR (D180–R190).

enzymatic activity of MCM resulting in methylmalonic aciduria.^{7,14,15}

Structure–function studies on PduO-type ATRs from *Lactobacillus reuteri*^{16–19} and *Methylbacterium extorquens*^{13,20,21} have provided mechanistic insights into these enzymes. Cob(II) alamin binds to ATR in a “base-off” conformation in which the lower axial DMB base is displaced from the cobalt ion.^{22,23} A yet unknown mitochondrial oxidoreductase catalyzes the one electron reduction of mammalian ATR-bound cob(II)alamin, yielding cob(I)alamin²⁴ (eq 1).



Cob(I)alamin is a potent nucleophile and attacks the C-5′ ribosyl carbon of ATP forming PPPi and AdoCbl, which is “base-off” and five-coordinate.^{16,25,26} In contrast, AdoCbl bound to MCM is in a six-coordinate “base-off/His-on” conformation in which a histidine residue donated by MCM occupies the lower axial position.¹ This difference in coordination number results in large differences in the absorption spectra and is experimentally useful for locating the cofactor.¹³ Thus, “base-off” AdoCbl bound to ATR

exhibits an absorbance maximum at 458 nm while “base-off/His-on” AdoCbl bound to MCM or free in solution has a maximum at 525 nm.¹³

PduO-type ATR is a homotrimer that appears to use only two of its three active sites at a time and exhibits negative cooperativity for substrate and product binding.^{13,20,27} In the crystal structure of human PduO-type ATR, 2 equiv of ATP are bound per homotrimer.²⁸ ATP binding to the vacant site in the *M. extorquens* ATR triggers ejection of only 1 of 2 equiv of AdoCbl, providing a mechanism for driving transfer to MCM in what has been described as a “rotary mechanism” (Figure 1).²⁷ However, the crystal structures of the *L. reuteri* ATR show occupancy of all three active sites with either ATP or cob(II)alamin.¹⁸ This difference may arise from altered behavior in the crystalline versus solution state or differences between PduO-type ATRs from different organisms. The apparent conservation of function between human and *M. extorquens* PduO-type ATR suggests that the *M. extorquens* ATR is a viable model for the human enzyme.

The ATR monomer comprises a five-helix bundle arranged in a head-to-tail fashion relative to the neighboring subunit. The active sites are located at the subunit interfaces (Figure 2).^{18,28} Residues at the N-terminus become ordered in response to ATP binding, and residues from the adjacent monomer contribute to the ATP binding site. Cobalamin binds in a C-terminal crevice, and backbone amides from the adjacent subunit participate in the majority of hydrogen-bonding interactions with the amide substituents on the corrin ring.¹⁸ Two conformational changes accompany binding of B₁₂: the ordering of the C-terminus and positioning of a mobile loop proximal to the lower axial face of B₁₂. This loop is hydrogen bonded to B₁₂, and its movement facilitates generation of four-coordinate cob(II)alamin.¹⁷ In contrast, the significance of the C-terminal ordering for ATR function is less well understood. Truncation of the final 16 residues in human ATR due to the nonsense Q234X mutation results in early onset methylmalonic aciduria.¹⁵ Structural studies on *LrPduO*-Δ183–188, an *L. reuteri* ATR missing the terminal six amino acids, revealed decreased conformational rigidity of the mobile loop, although cob(II)alamin was nonetheless bound in a four-coordinate “base-off” state.¹⁷ The *LrPduO*-Δ183–188 mutant exhibited a modest decrease in the catalytic efficiency relative to wild-type ATR, providing limited insight into the role of the C-terminal tail and the biochemical basis of pathogenicity of the Q234X patient mutation.¹⁷

In this study, we have mimicked the Q234X mutation in the *M. extorquens* ATR by introducing the D180X mutation, which corresponds to the site of the nonsense mutation in the human sequence (Figure 3). We demonstrate that while this C-terminal truncation has modest effects on the steady-state kinetic parameters, the affinity for the product, AdoCbl, and allosteric communication between active sites leading to negative cooperativity are adversely affected. These changes lead to corruption of the direct transfer mechanism of AdoCbl from ATR to MCM and provide insights into the importance of the C-terminal loop in gating cofactor transfer and for communication between adjoining active sites.

EXPERIMENTAL PROCEDURES

Materials. MANT-ATP (2′(3′)-O-(N-methylanthraniloyl)-ATP) was purchased from Jen Biosciences (Germany). ATP, AdoCbl, phenylmethylsulfonyl fluoride, lysozyme, and all other chemical

<i>M. extorquens</i>	-----MVKLNRITYT	9
<i>S. enterica</i>	-----MAITYT	5
<i>L. reuteri</i>	-----MKIYT	5
<i>H. sapien</i>	MAVCGLSRLGLGSRGLRGCFGAARLLYPRFQSRGPQGVEDGDRPQPSSKTPRIPKIYT	60
<i>B. taurus</i>	-----QSRGPQGVEDGDRPQPSSKTPKVPIYT	28
<i>M. extorquens</i>	RTGDOCTTGLANGERRSKADLRVEAYGTVDETNACTGLAR-LTAEPA--LDAMLARIQND	66
<i>S. enterica</i>	RTGDAGTSLFTGQRVSKTHPRVEAYGTLDELNAALSLCACAAADEN--HRTLEAIIQQQ	63
<i>L. reuteri</i>	KNGDKGQTRIIGKOILYKNDPRVAAYGEVDELNSWVGYSKSLINSHTQVLSNEEEIIQQL	65
<i>H. sapien</i>	KTGDKGFSSTFTGERRPKDDQVFEAVGTTDELSSAIGFALELVTEKGHTFAEELQKIQCT	120
<i>B. taurus</i>	KTGDKGFSSTFTGERRSKDDQVFEAVGTTDELSSAIGFAMELIAEKGHFPVEELQKIQCS	88
<i>M. extorquens</i>	LFDLGADLATPP-SDKPLGYEPLRIVPAQVQRLETEIDALNANIPPLKSFVLPGGSAAAA	125
<i>S. enterica</i>	LFWFSABELSD--SEQPS-PKQRYISSEEISALEAAIDRAMARVEPLHSFILPGRCEAAS	120
<i>L. reuteri</i>	LFDCGHDLATPA-DDERHSFKFKQEQP--TVWLEEKIDNYTQVPAVKKFIPLPGGTQLAS	122
<i>H. sapien</i>	LQDVGSALATPCSSAREAHLYKTTTFKAGPILELEQWIDKYTSQPLPLTAFILPSSGKISS	180
<i>B. taurus</i>	LQDVGSALATPRSSAREAHLYKATFEAGPILELEQWIDKYSRQLPPLTAFILPSSGKSSS	148
<i>M. extorquens</i>	ALHLARTVCRRARERLVVALSGVESEAISGEALQYINRLSDFLFVASRAAN-----R	176
<i>S. enterica</i>	RLHFARTLARRAERRLVELA--TEVNVRQVLMRYINRLSDCLYALARAEDSDAHQANIIR	178
<i>L. reuteri</i>	ALHVARTITTRARERQIVOLMR--EEQINQDVLIFINRLSDYTFAAARYAN-----YL	172
<i>H. sapien</i>	ALHFCRAVCRRARERVPLVQMGETDAN--VAKFLNRLSDYLEFTLARYAA-----MK	230
<i>B. taurus</i>	ALHFCRAVCRRARERVPLVQGETDAN--VVKFLNRLSDYLEFTLARYTA-----MK	198
<i>M. extorquens</i>	* DGADDVWVPGQNR-----	190
<i>S. enterica</i>	EVSKRYLAASQPTR-----	192
<i>L. reuteri</i>	EQQPDMEYRNSKDVFR----	188
<i>H. sapien</i>	EGNQEKLYMKNDPSAESEGL	250
<i>B. taurus</i>	EGNPEKLYKKNDSLDRT---	215

Figure 3. Sequence comparison of select PduO-type ATRs. Multiple sequence alignment of PduO-type ATRs in which amino acids that are identical (black) or conserved (gray) are highlighted. The sequence of the human ATR includes an N-terminal 32 amino acid mitochondrial leader sequence. An asterisk indicates the position of residue D180.

reagents were purchased from Sigma. The Stratagene Quikchange II XL Site-Directed Mutagenesis Kit was purchased from Agilent.

Construction of the D180X ATR Mutant. The mutation was created using the Quikchange kit and the following primers: sense: 5'-CAACCGCGACGCGCCTAGGACGTGCTCTGGTG-3' and an antisense primary containing the complementary sequence. The 6xHis-wild-type ATR expression plasmid described previously²⁰ was used as template. The mutation was confirmed by nucleotide sequence determination at the University of Michigan DNA Sequencing Core.

Expression and Purification of ATR. *Escherichia coli* (BL21 (DE3)) was transformed with plasmids encoding recombinant D180X ATR or 6xHis-wild-type ATR and grown at 37 °C in 1 L of Luria–Bertani media containing kanamycin (50 µg/mL). Cultures were grown to an optical density at 600 nm of 0.5–0.6 and induced with either 0.1 mM (for D180X ATR) or 1 mM (for wild-type ATR) isopropyl-β-D-thiogalactopyranoside. Cultures were then grown at 20 °C for 14–16 h (D180X ATR) or at 37 °C for 6–10 h (wild-type ATR) prior to harvesting.

ATR (wild-type and D180X) was purified as follows. Bacterial pellets were suspended in 50 mM sodium phosphate buffer, pH 8.0, containing 0.3 M KCl, 20 mM imidazole, and 1 mM phenylmethylsulfonyl fluoride (buffer A). Cells were lysed first by treatment with lysozyme (25 mg/L culture; 40 000 U/mg) for 1 h with stirring at 4 °C and then disrupted by sonication as described previously.²⁰ The pellet was separated by centrifugation at 19000g at 4 °C. The supernatant was filtered through a 0.4 µm syringe filter and diluted to 4–5 mg protein/mL before loading onto a 50 mL nickel–nitrilotriacetic acid–Sepharose column pre-equilibrated with 10–20 column volumes of buffer

A. The column was washed with 10 column volumes of buffer A and eluted with a linear gradient of 20–300 mM imidazole in buffer A. Fractions containing the target protein were pooled, concentrated, dialyzed extensively against 50 mM HEPES, pH 8, 0.3 M KCl, 5% glycerol (buffer B) at 4 °C, and then dialyzed extensively against buffer B containing 10 mM MgCl₂ at 4 °C. This purification protocol typically yielded 15–20 mg of ≥95% pure protein per liter of culture.

ATR Activity Assays. ATR activity was monitored in a steady-state assay as described previously,²⁰ and data were fit to the Michaelis–Menten equation to obtain the kinetic parameters. The *K_M* for ATP was determined at saturating HOCbl (55 µM) and varying ATP (from 0.5 to 300 µM). The *K_M* for HOCbl was determined at saturating ATP (1 mM) and varying HOCbl (from 0.5 to 60 µM) concentrations.

Thermal Denaturation Assays. Thermal denaturation of ATR was performed to assess the relative stabilities of the wild-type and mutant proteins. For this, 0.5 mg/mL of purified ATR in buffer B containing 10 mM MgCl₂ was placed in a cuvette, and the temperature was increased from 4 to 68 °C in a Cary 100 Bio UV/vis spectrophotometer with a heating block connected to a Fisher Scientific Isotemp 3016S water bath. Unfolding was measured by increased light scattering at 600 nm in 5 °C increments until no further change in the optical density was observed. Data were analyzed as described previously.²⁹

Isothermal Titration Calorimetry (ITC). ITC experiments were performed as described previously^{13,30} with the exception that the temperature was maintained at 4 °C due to the instability of D180X ATR at ambient temperature for prolonged periods. ITC experiments, conducted in triplicate, were analyzed with

MicroCal ORIGIN software to determine the bimolecular association constant (K_A), binding enthalpy (ΔH°), and binding entropy (ΔS°). Briefly, 40–45 μM D180X ATR in 50 mM HEPES, 0.3 M KCl, 10 mM MgCl_2 , 5% glycerol at pH 8 was titrated with 45 μL aliquots of 1–2 mM ATP or AdoCbl. Following integration of the calorimetric signals in MicroCal ORIGIN software, ITC data for the titration of D180X ATR with ATP were fitted to a two-sites model that describes two populations of active sites that bind ATP with distinct thermodynamic parameters. When D180X ATR was titrated with AdoCbl, a single-site model was used to fit the data. The Gibbs free energy of binding either ligand was calculated using eqs 2 and 3.

$$\Delta G^\circ = -RT \ln(K_A) \quad (2)$$

$$\Delta G^\circ = \Delta H^\circ - T\Delta S^\circ \quad (3)$$

Fluorescence and UV/vis Titrations. For the UV/vis titration of AdoCbl with D180X ATR, experiments were performed in quadruplicate, and the large hypsochromic shift from 525 to 458 nm associated with the “base-on” to “base-off” transition for AdoCbl was used to monitor binding. Titrations were performed at 4 $^\circ\text{C}$, and all stock solutions were kept chilled throughout the experiment. Briefly, 1.5–10 μM AdoCbl in 50 mM HEPES, pH 8 containing 0.3 M KCl, 10 mM MgCl_2 and 5% glycerol was titrated with 1–100 μM D180X ATR in the same buffer. Spectra were recorded 8–10 min after each addition of enzyme to allow binding to reach equilibrium. Data were fit to a hyperbolic binding isotherm to determine the dissociation constant, K_D , for binding of AdoCbl to D180X ATR. For wild-type ATR, titrations were performed using 4 μM enzyme +8 μM AdoCbl and aliquots of a 1 mM ATP stock solution. The corresponding titration with D180X ATR was performed using 130 μM enzyme, 2 μM AdoCbl, and aliquots of a 20 mM ATP stock solution. Titrations of MANT-ATP with D180X were monitored via the quenching of MANT fluorescence upon binding. Briefly, 10–15 μM of MANT-ATP in 50 mM HEPES, 0.3 M KCl,

10 mM MgCl_2 , 5% glycerol at pH 8 was titrated with 100 μM D180X ATR in the same buffer to a final concentration of 35 μM protein at 4 $^\circ\text{C}$. Fluorescence quenching was monitored at 444 nm (360 nm excitation), and its dependence on D180X ATR concentration was fitted to a hyperbolic binding isotherm. The MANT-ATP titrations were performed in triplicate.

RESULTS

Stability of Wild-Type and D180X ATR. During purification, the stability of the D180X mutant was noted to be lower than for wild-type ATR, as evidenced by precipitation especially during concentration. Comparison of the thermal denaturation profiles confirmed that the D180X mutant is indeed less stable relative to wild-type ATR with a $\Delta T_m = 11.1 \pm 0.4$ $^\circ\text{C}$ (Figure 4).

Kinetic Characterization of Wild-Type and D180X ATR. The initial velocity of the adenosylation reaction was monitored at 390 nm (corresponding to conversion of cob(I)alamin to AdoCbl) by varying the concentration of cob(I)alamin at saturating concentrations of ATP, or vice versa (Table 1). The apparent K_M^{ATP} (8.4 ± 1.4 μM) for wild-type ATR is similar to previously reported values for the N-terminally His₈-tagged human (K_M , 7.2 μM) and *L. reuteri* (K_M , 2 μM) ATRs. Similarly, the $K_M^{\text{cob(I)}}$ for wild-type ATR is similar to values reported for other PduO-type ATRs (K_M , 0.2–5 μM ^{8,31–33}) but 5-fold lower than the value reported for His-tagged human ATR.³¹ The k_{cat} for wild-type *M. extorquens* ATR is 4-fold larger than any value previously reported for a PduO-type ATR.

The D180X mutation has modest effects on the steady-state kinetic parameters: $K_M^{\text{cob(I)}}$ and k_{cat} are 2- and 3.5-fold smaller, respectively, resulting in a 7-fold lower catalytic efficiency with respect to the cob(I)alamin substrate (Table 1). The K_M for ATP is unaffected by the D180X mutation.

Thermodynamic Characterization of ATP and AdoCbl Binding. Binding of ATP to D180X ATR was characterized by ITC and by fluorescence spectroscopy using MANT-ATP (Figure 5A). A monophasic binding isotherm was obtained from the fluorescence titration and yielded a K_D value of 5.4 ± 1.1 μM for binding of MANT-ATP to D180X ATR. This value is comparable to the K_D value of 5.9 ± 1.4 μM reported for binding of the second equivalent of ATP to wild-type ATR.²⁷ In contrast, ITC data for ATP binding to D180X ATR exhibits biphasic behavior (Figure 5B). The discrepancy between the fluorescence and ITC data may be derived from the low amplitude of fluorescence quenching upon binding of MANT-ATP to site 1 and is consistent with prior data on MANT-ATP binding to ATR by stopped-flow fluorescence spectroscopy.²⁷

Analysis of the ITC data yielded ΔG_1° and ΔG_2° values of -8.1 kcal/mol and -6.9 kcal/mol for binding of ATP to sites 1 and 2 in D180X ATR (Table 2), which are virtually identical to those reported for wild-type ATR (-8.3 kcal/mol and -6.6 kcal/mol, respectively). However, the relative contributions of the entropic and enthalpic terms to the ΔG° values differ

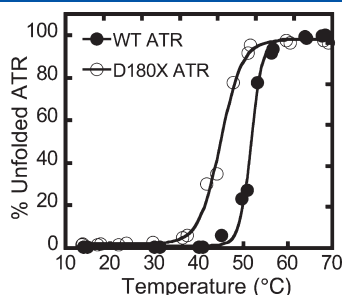


Figure 4. Thermal melting curves for wild-type ATR (filled circles) and D180X ATR (open circles). Plots were normalized to the maximum turbidity observed at 600 nm. Protein unfolding was monitored as described under Experimental Procedures.

Table 1. Kinetic Parameters of Wild-Type and D180X ATR^a

enzyme	k_{cat} (s^{-1})	ATP dependence		Cob(I)alamin dependence	
		K_M (μM)	k_{cat}/K_M ($\text{M}^{-1} \text{s}^{-1}$)	K_M (μM)	k_{cat}/K_M ($\text{M}^{-1} \text{s}^{-1}$)
wild type	$(8.9 \pm 0.1) \times 10^{-1}$	8.4 ± 1.4	$(5.0 \pm 0.3) \times 10^4$	0.4 ± 0.1	$(2.5 \pm 0.2) \times 10^6$
D180X	$(2.5 \pm 0.1) \times 10^{-1}$	9.5 ± 1.2	$(2.7 \pm 0.1) \times 10^4$	0.8 ± 0.1	$(3.5 \pm 0.1) \times 10^5$

^aThe values represent the mean \pm SD from at least three independent experiments in the adenosylation reaction.

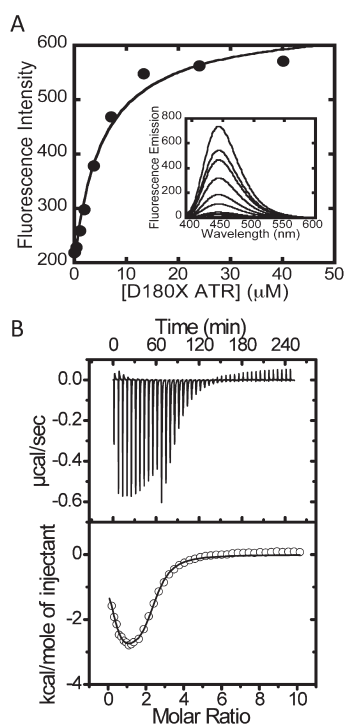


Figure 5. Binding of ATP to D180X ATR. (A) The inset shows a representative fluorescence titration of MANT-ATP (15 μM) with D180X ATR (0–40 μM) at 10 $^{\circ}\text{C}$. (B) Representative calorimetric titration data for binding of ATP to ATR (50 μM) in buffer B at 4 $^{\circ}\text{C}$. The top panel depicts the raw data for ATP binding in power versus time. The lower panel shows integration of data in the top panel, which is proportional to the heat release that accompanies binding as a function of time. The data in the lower panel were best fit to a two-sites binding model and yielded the thermodynamic parameters that govern ATP binding to D180X ATR at 4 $^{\circ}\text{C}$ (shown in Table 2).

between the D180X mutant and wild-type ATR. Thus, binding of ATP to sites 1 and 2 is enthalpically dominated ($\Delta H_1^{\circ} = -8.1$ kcal/mol and $\Delta H_2^{\circ} = -6.0$ kcal/mol) in wild-type ATR, while it is entropically driven in the D180X mutant ($T\Delta S_1^{\circ} = 7.9$ kcal/mol and $T\Delta S_2^{\circ} = 3.4$ kcal/mol).

Binding of AdoCbl is significantly impacted in the D180X mutant, which exhibits a K_D^{AdoCbl} of 71 ± 24 μM (Figure 6A) in comparison to the 0.1 and 2.0 μM values for sites 1 and 2 reported for the wild-type enzyme.²⁷ The relatively low affinity of the D180X mutant for AdoCbl necessitated high protein concentrations during spectrophotometric titrations and was limited by the instability of the mutant protein. Hence, only $\sim 83\%$ saturation with AdoCbl could be observed in the spectrophotometric binding assay (Figure 6A). In principle, the inability to observe binding of 2 equiv of AdoCbl in the “base-off” state per trimer could arise from two possibilities: (i) only 1 equiv of AdoCbl binds to the D180X mutant in the “base-off” conformation while the second equivalent binds in the “base-on” conformation and (ii) the dissociation constant for AdoCbl binding at site 2 is $\gg 70$ μM measured by spectral titration. To distinguish between these possibilities, AdoCbl binding was also monitored by ITC (Figure 6B). The calorimetric titrations showed monophasic behavior for AdoCbl binding, and the data were best fit to a single-binding site model with $N = 2$ per ATR homotrimer (Table 2). The ITC data confirm that AdoCbl binds to D180X ATR with an ~ 700 - and 35-fold weaker binding affinity at sites 1

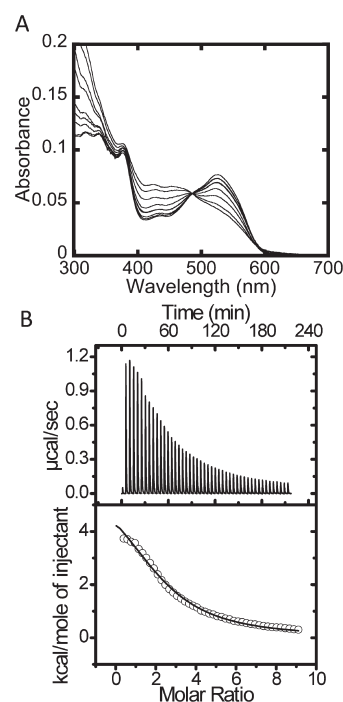


Figure 6. Binding of AdoCbl to D180X ATR. (A) The UV/vis spectra were obtained by titrating a fixed concentration of AdoCbl (7.5 μM) with increasing concentrations of D180X ATR (0–150 μM). Approximately 83% saturation of the two AdoCbl binding sites per trimer was achieved based on $\Delta\epsilon_{525} = 6.69 \text{ M}^{-1} \text{ cm}^{-1}$. (B) Representative ITC data for binding of AdoCbl to D180X ATR (50 μM) in buffer B at 4 $^{\circ}\text{C}$. The top panel depicts the raw data for AdoCbl-binding in power versus time. The lower panel shows integration of data in the top panel. The data in the lower panel were best fit to a single-site binding model and gave the thermodynamic parameters associated with binding of AdoCbl to D180X ATR at 4 $^{\circ}\text{C}$.

and 2 compared to wild-type enzyme. Hence, the C-terminal deletion leads to loss of negative cooperativity associated with AdoCbl binding to wild-type ATR.

Corruption of the ATP-Triggered Mechanism for AdoCbl Unloading. A characteristic of AdoCbl transfer from ATR to MCM is the ATP-stimulated ejection of 1 equiv of AdoCbl from ATR (Figure 1).²⁰ To determine whether ATP triggers product release irrespective of whether one or two AdoCbl molecules are bound, wild-type ATR was loaded under conditions where a vast excess of active sites over AdoCbl (i.e., 100:1) resulted statistically, in the predominance of the 1:1 ATR:AdoCbl complex. Addition of 0–30 mM ATP to this complex (corresponding to a 0–200-fold excess of ATP over ATR) failed to trigger release of AdoCbl into solution, demonstrating that binding of ATP only releases AdoCbl from the low affinity site when 2 equiv of AdoCbl are bound (Figure 7).

Next, the fidelity of the ATP-dependent AdoCbl release mechanism was assessed in the D180X mutant. The spectrum obtained upon mixing AdoCbl with a 50-fold excess of D180X ATR indicates that at least 85% of the cofactor is bound in the “base-off” conformation (Figure 8). The low affinity and equivalence of AdoCbl binding to sites 1 and 2 in D180X ATR results in a statistical distribution of populations with 0, 1, or 2 equiv of AdoCbl bound per ATR trimer. Addition of 5 mM ATP to this sample resulted in full displacement of all bound AdoCbl into solution as evidenced by the appearance of the “base-on”

Table 2. Thermodynamic Parameters for Binding of ATP and AdoCbl to D180X ATR

	ATP ^a		AdoCbl ^b
	site 1	site 2	sites 1 and 2
K_D (μ M)	0.48 ± 0.02	4.01 ± 0.61	44.1 ± 3.2
ΔH° (kcal/mol)	-0.27 ± 0.02	-3.40 ± 0.04	5.61 ± 0.26
$T\Delta S^\circ$ (kcal/mol)	7.86 ± 0.91	3.41 ± 0.04	11.10 ± 0.63
ΔG°	-8.12 ± 0.90	-6.87 ± 0.61	-5.49 ± 0.89
N^c (sites)	0.38 ± 0.08	1.43 ± 0.07	2.07 ± 0.07

^a ITC data for ATP binding were fitted to a two-site model. ^b The isotherms for binding of AdoCbl to D180X ATR were best fit to a single-binding-site model. ^c N represents the number of unique sites described by the fitting model.

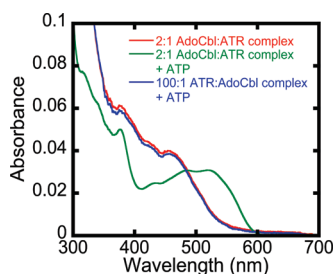


Figure 7. ATP-triggered release of AdoCbl only from the low affinity site in wild-type ATR. The difference in K_D s for the two AdoCbl sites on ATR implies that when $[ATR] \gg [AdoCbl]$, site 2 is predominantly vacant and site 1 is occupied. Spectrum A is that of “base-off” AdoCbl in the 2:1 (AdoCbl·wild-type ATR) complex where the concentration of AdoCbl is identical to the concentration of AdoCbl-binding sites. Spectrum C is the spectrum after addition of 30 mM ATP to spectrum A (i.e., ~50% bound AdoCbl is released into solution upon addition of ATP). Spectrum B is of “base-off” AdoCbl when AdoCbl·ATR is 1:100 in the presence of 30 mM ATP. ATP is unable to stimulate release of AdoCbl under these conditions when only the high affinity binding site in ATR is occupied by AdoCbl and the low affinity site is vacant. Titrations were performed at 4 °C and recorded after 20 min to allow binding equilibration.

spectrum. The presence of free AdoCbl in solution was confirmed by separation using a Centricon filter.

DISCUSSION

In this study, we have mimicked the pathogenic Q243X truncation found in human ATR¹⁷ to assess the role of the C-terminal tail in AdoCbl synthesis and transfer to MCM. AdoCbl levels are reduced ~70% in cultured fibroblasts harboring the Q234X deletion, and supplementation with exogenous B₁₂ provides only mild stimulation of MCM activity.¹⁵ The corresponding *M. extorquens* D180X mutant exhibits lower protein stability (Figure 4), and the steady-state kinetic parameters for adenosylation of cob(I)alamin are only modestly impacted (Table 1). The steady-state kinetic parameters of the *LrPduO*ΔS183–188 mutant, designed to mimic the Q243X mutation in the human sequence, are similarly mildly affected compared to wild-type ATR. These results suggest that the C-terminus does not play a critical role in synthesis of AdoCbl at least under *in vitro* conditions.¹⁷ However, as indicated by both the primary sequence alignment and the crystal structure of the *LrPduO* ATR holoenzyme, residue P176 of *LrPduO*, and not residue S183, corresponds to Q234 in the human sequence. Hence, the *LrPduO*ΔS183–188 sequence represents a shorter

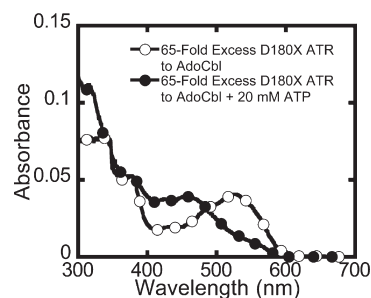


Figure 8. Corruption of the ATP-dependent mechanism for release of a single equivalent of AdoCbl in the D180X mutant. Mixing AdoCbl with a 65-fold excess of D180X ATR generated the spectrum (filled circles) with ~90% bound AdoCbl at 4 °C in buffer B. Because of the equivalence of sites 1 and 2 for AdoCbl binding in D180X ATR, the spectrum represents a statistical distribution of ATR with 0, 1, or 2 equiv of AdoCbl bound at the active site. Addition of 20 mM ATP resulted in the complete displacement of AdoCbl from D180X ATR (open circles). Thus, whereas ATP is only capable of displacing AdoCbl from the low affinity site in wild-type ATR when 2 equiv of AdoCbl are bound, the D180X mutant binds AdoCbl with equal and low affinity at both binding sites and ejects both equivalents of AdoCbl in response to ATP binding.

C-terminal truncation than that resulting from the human Q234X mutation. Importantly, while the wild-type *LrPduO* gene can rescue the growth of a ΔCobA strain of *S. enterica* on minimal media, *LrPduO*ΔS183–188 is unable to do so. This is consistent with our results on the *M. extorquens* D180X mutant, which reveal that the C-terminal truncation impairs AdoCbl transfer from ATR to MCM rather than AdoCbl synthesis *per se*.

In the structure of the *L. reuteri* ATR, cobalamin is bound in a hydrophobic cavity that is capped by an ordered C-terminal tail.¹⁸ Modeling the corresponding Q234X mutation into the *LrPduO* ATR structure suggests loss of the C-terminal cap of the B₁₂ binding site (Figure 9). Thus, a predicted outcome of the Q234X mutation is weaker binding of AdoCbl, which is borne out by the significant reduction in the affinity of the D180X mutant for AdoCbl (Table 2).

The C-terminal truncation is also predicted to lead to loss of key hydrogen-bonding interactions with AdoCbl and the mobile loop (Figure 10A). In the structure of *LrPduO* holoenzyme, residues R188, V186, and K184 participate in either direct or water-mediated hydrogen bonds, via backbone amides with the amide substituents of the corrin ring (Figure 10).¹⁸ The low C-terminal sequence conservation among the PduO-type ATRs from different organisms is likely due to the use of backbone amides rather than side chains for hydrogen bonding.

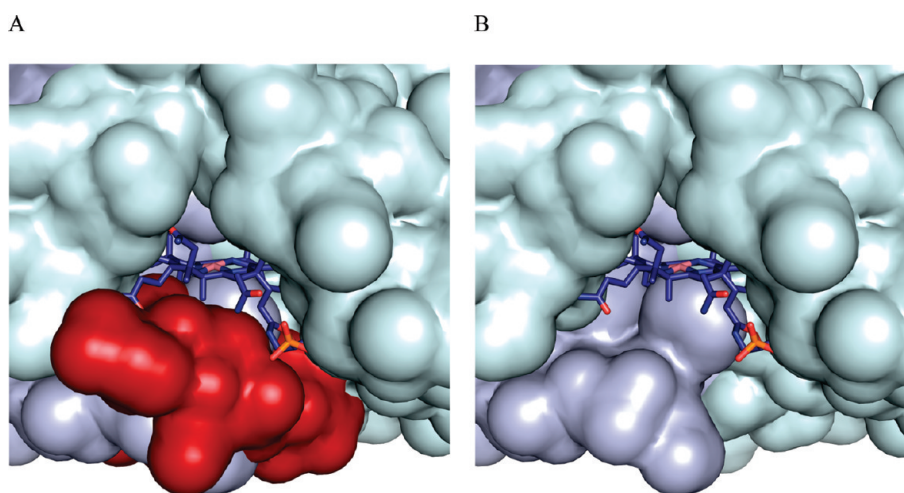


Figure 9. Surface representation of the cobalamin binding site in ATR. (A) Cob(II)alamin is shown in stick representation, while adjacent subunits colored as in Figure 2 are shown in surface representation. The C-terminal loop residues deleted in the D180X mutant are shown in red in (A) and are deleted in (B). The figure was created using the PDB file 3CI4.

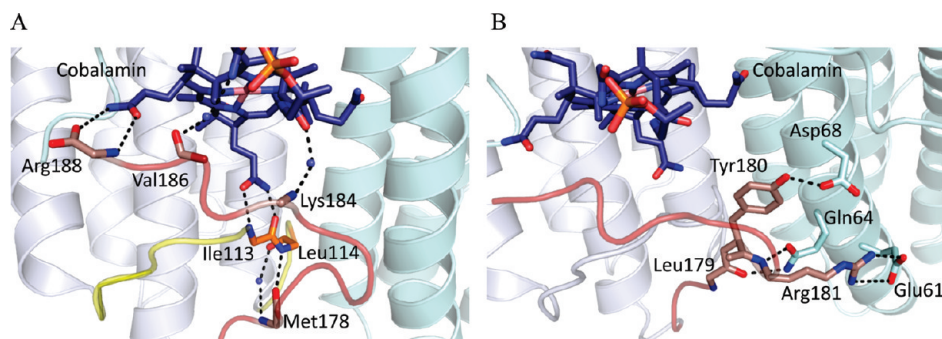


Figure 10. Map of interactions between cob(II)alamin and *LrPduO* ATR. (A) Shown are the intermolecular hydrogen-bonding interactions formed between the peptide backbone of the C-terminus with cobalamin and the peptide backbone of the mobile loop. All side chains have been excluded for clarity. The C-terminal loop missing in the D180X mutant is shown in red, and the backbone of residues M178, K184, V186, and R188 are shown as sticks. The mobile loop is shown in yellow, and the amide backbone of residues I113 and L114 are indicated. Hydrogen bond interactions are depicted as black dashes. (B) Shown are the proposed allosteric contacts between residues of the C-terminus in one subunit and helix 2 residues on the adjacent subunit. The C-terminus and residues L179, Y180, and R181, shown as sticks, are colored red. For clarity, only the amide backbone of L179 is shown. Residues E61, Q64, and D68 of the adjacent subunit are shown as sticks. Cobalamin is colored dark blue and shown in stick representation.

Additionally, ordering of the C-terminus triggers the formation of hydrogen-bonding contacts between B₁₂ and residues I113 and L114 in the mobile loop. Thus, while ordering of the C-terminus may contribute to orienting the mobile loop over the lower face of cobalamin, it is not required for generating “base-off” AdoCbl.

It is unclear how the C-terminal truncation leads to loss of allosteric communication between adjacent active sites. The binding of ATP to the vacant site in the wild-type ATR·2AdoCbl product complex triggers ejection of only a single equivalent of AdoCbl, presumably from the low affinity site (Figure 7). In D180X ATR, the two binding sites are equivalent, and both display low affinity for AdoCbl. Binding of ATP leads to release of both equivalents of AdoCbl from the trimer (Figures 6 and 8). Comparison of the apo- and holo-*LrPduO* crystal structures suggests a possible mechanism for signal transmission between neighboring subunits.^{16,18,19} B₁₂ binding induces interactions between the C-terminus of one subunit and helix 2 residues in the adjacent subunit (Figure 10B). These interactions include a salt

bridge between R181 in the C-terminus and E61 and a hydrogen bond network between the side chains of residues D68 and Q64 and peptide backbone of R181 and L179 and the phenolic oxygen of Y180 in the neighboring C-terminus.¹⁸ A two amino acid deletion of helix 2 residues in the human sequence I117-Q118del results in methylmalonic aciduria. Although this deletion mutation has been found in a compound heterozygous state, i.e., the other ATR allele carries a different mutation, it would be of interest to further investigate the importance of this deletion mutation and other helix 2 residues in allosteric communication.¹⁴

In summary, our studies on the *M. extorquens* D180X mutation designed to mimic the patient Q243X mutation provide insights into the functions of ATR not only as an enzyme but also as an escort responsible for conveying AdoCbl to the client enzyme, MCM. The observations of decreased MCM activity and lower AdoCbl levels in the Q234X patient cell lines this study. We propose that the lower AdoCbl levels in patient fibroblasts likely reflect a combination of instability of the Q234X mutant and weaker affinity for cobalamin. Supplementation of fibroblasts

that are homozygous for the Q234X mutation with OHcbl leads to a modest increase in MCM activity and may result from an increased free AdoCbl pool, which facilitates reconstitution of MCM.

AUTHOR INFORMATION

Corresponding Author

*Tel: (734) 615-5238; Fax: (734) 647-6180; e-mail: rbanerje@umich.edu.

Funding Sources

This work was supported in part by grants from the National Institutes of Health (DK45776 and GM007767).

ACKNOWLEDGMENT

We thank Tanya Labunska (University of Nebraska) for generating the *M. extorquens* D180X ATR mutant and Dr. Dominique Padovani for his early guidance in this work.

ABBREVIATIONS

AdoCbl, 5'-deoxyadenosylcobalamin or coenzyme B₁₂; ATR, adenosyltransferase; MANT-ATP, (2'(3')-O-(N-methylanthraniloyl) adenosine 5'-triphosphate; ITC, isothermal titration calorimetry; D180X ATR, ATR from *Methylobacterium extorquens* AM1 truncated at Asp180; DMB, dimethylbenzimidazole; MCM, methylmalonyl-CoA mutase; HOcbl, hydroxocobalamin.

REFERENCES

- (1) Banerjee, R., and Ragsdale, S. W. (2003) The many faces of vitamin B₁₂: catalysis by cobalamin-dependent enzymes. *Annu. Rev. Biochem.* 72, 209–247.
- (2) Bandarian, V. a. R., G. H. (1999) Ethanolamine ammonia-lyase in *Chemistry and Biochemistry of B₁₂* (Banerjee, R., Ed.) Wiley, New York.
- (3) Banerjee, R. a. C. S. (1999) Methylmalonyl-CoA mutase in *Chemistry and Biochemistry of B₁₂* (Banerjee, R., Ed.), Wiley, New York.
- (4) Mera, P. E., and Escalante-Semerena, J. C. (2010) Multiple roles of ATP:cob(I)alamin adenosyltransferases in the conversion of B₁₂ to coenzyme B₁₂. *Appl. Microbiol. Biotechnol.* 88, 41–48.
- (5) Tsang, A. W., and Escalante-Semerena, J. C. (1996) cobB function is required for catabolism of propionate in *Salmonella typhimurium* LT2: evidence for existence of a substitute function for CobB within the 1,2-propanediol utilization (pdu) operon. *J. Bacteriol.* 178, 7016–7019.
- (6) Suh, S., and Escalante-Semerena, J. C. (1995) Purification and initial characterization of the ATP:corrinoid adenosyltransferase encoded by the cobA gene of *Salmonella typhimurium*. *J. Bacteriol.* 177, 921–925.
- (7) Dobson, C. M., Wai, T., Leclerc, D., Kadir, H., Narang, M., Lerner-Ellis, J. P., Hudson, T. J., Rosenblatt, D. S., and Gravel, R. A. (2002) Identification of the gene responsible for the *cblB* complementation group of vitamin B₁₂-dependent methylmalonic aciduria. *Hum. Mol. Genet.* 11, 3361–3369.
- (8) Leal, N. A., Park, S. D., Kima, P. E., and Bobik, T. A. (2003) Identification of the human and bovine ATP:Cob(I)alamin adenosyltransferase cDNAs based on complementation of a bacterial mutant. *J. Biol. Chem.* 278, 9227–9234.
- (9) Banerjee, R. (2006) B₁₂ trafficking in mammals: A for coenzyme escort service. *ACS Chem. Biol.* 1, 149–159.
- (10) Banerjee, R., Gherasim, C., and Padovani, D. (2009) The Tinker, Tailor, Soldier in intracellular B₁₂ Trafficking. *Curr. Opin. Chem. Biol.* 13, 477–484.
- (11) Kim, J., Hannibal, L., Gherasim, C., Jacobsen, D. W., and Banerjee, R. (2009) A human vitamin B₁₂ trafficking protein uses

glutathione transferase activity for processing alkylcobalamins. *J. Biol. Chem.* 284, 33418–33424.

(12) Kim, J., Gherasim, C., and Banerjee, R. (2008) Decyanation of vitamin B₁₂ by a trafficking chaperone. *Proc. Natl. Acad. Sci. U.S.A.* 105, 14551–14554.

(13) Padovani, D., Labunska, T., Palfey, B. A., Ballou, D. P., and Banerjee, R. (2008) Adenosyltransferase tailors and delivers coenzyme B₁₂. *Nat. Chem. Biol.* 4, 194–196.

(14) Jorge-Finnigan, A., Aguado, C., Sanchez-Alcudia, R., Abia, D., Richard, E., Merinero, B., Gamez, A., Banerjee, R., Desviat, L. R., Ugarte, M., and Perez, B. (2010) Functional and structural analysis of five mutations identified in methylmalonic aciduria *cblB* type. *Hum. Mutat.* 31, 1033–1042.

(15) Lerner-Ellis, J. P., Gradinger, A. B., Watkins, D., Tirone, J. C., Villeneuve, A., Dobson, C. M., Montpetit, A., Lepage, P., Gravel, R. A., and Rosenblatt, D. S. (2006) Mutation and biochemical analysis of patients belonging to the *cblB* complementation class of vitamin B₁₂-dependent methylmalonic aciduria. *Mol. Genet. Metab.* 87, 219–225.

(16) Mera, P. E., St, Maurice, M., Rayment, I., and Escalante-Semerena, J. C. (2007) Structural and functional analyses of the human-type corrinoid adenosyltransferase (PduO) from *Lactobacillus reuteri*. *Biochemistry* 46, 13829–13836.

(17) Mera, P., St, Maurice, M., Rayment, I., and Escalante-Semerena, J. (2009) Residue Phe112 of the Human-type Corrinoid Adenosyltransferase (PduO) Enzyme of *Lactobacillus reuteri* is Critical to the Formation of the Four-coordinate Co(II) Corrinoid Substrate and to the Activity of the Enzyme. *Biochemistry* 48, 3138–3145.

(18) St Maurice, M., Mera, P., Park, K., Brunold, T. C., Escalante-Semerena, J. C., and Rayment, I. (2008) Structural characterization of a human-type corrinoid adenosyltransferase confirms that coenzyme B₁₂ is synthesized through a four-coordinate intermediate. *Biochemistry* 47, 5755–5766.

(19) St Maurice, M., Mera, P. E., Taranto, M. P., Sesma, F., Escalante-Semerena, J. C., and Rayment, I. (2007) Structural characterization of the active site of the PduO-type ATP:Co(I)rrinoid adenosyltransferase from *Lactobacillus reuteri*. *J. Biol. Chem.* 282, 2596–2605.

(20) Padovani, D., and Banerjee, R. (2009) A Rotary Mechanism for Coenzyme B₁₂ Synthesis by Adenosyltransferase. *Biochemistry* 48, 5350–5357.

(21) Padovani, D., and Banerjee, R. (2009) A G-protein editor gates coenzyme B₁₂ loading and is corrupted in methylmalonic aciduria. *Proc. Natl. Acad. Sci. U.S.A.* 106, 21567–21572.

(22) Stich, T. A., Buan, N. R., Escalante-Semerena, J. C., and Brunold, T. C. (2005) Spectroscopic and computational studies of the ATP:corrinoid adenosyltransferase (CobA) from *Salmonella enterica*: insights into the mechanism of adenosylcobalamin biosynthesis. *J. Am. Chem. Soc.* 127, 8710–8719.

(23) Stich, T. A., Yamanishi, M., Banerjee, R., and Brunold, T. C. (2005) Spectroscopic evidence for the formation of a four-coordinate Co²⁺ cobalamin species upon binding to the human ATP:cobalamin adenosyltransferase. *J. Am. Chem. Soc.* 127, 7660–7661.

(24) Mera, P. E., and Escalante-Semerena, J. C. (2010) Dihydroflavin-driven adenosylation of 4-coordinate Co(II) corrinoids: are cobalamin reductases enzymes or electron transfer proteins? *J. Biol. Chem.* 285, 2911–2917.

(25) Park, K., Mera, P. E., Escalante-Semerena, J. C., and Brunold, T. C. (2008) Kinetic and spectroscopic studies of the ATP:corrinoid adenosyltransferase PduO from *Lactobacillus reuteri*: substrate specificity and insights into the mechanism of Co(II)corrinoid reduction. *Biochemistry* 47, 9007–9015.

(26) Yamanishi, M., Labunska, T., and Banerjee, R. (2005) Mirror “base-off” conformation of coenzyme B₁₂ in human adenosyltransferase and its downstream target, methylmalonyl-CoA mutase. *J. Am. Chem. Soc.* 127, 526–527.

(27) Padovani, D., and Banerjee, R. (2009) A rotary mechanism for coenzyme B(12) synthesis by adenosyltransferase. *Biochemistry* 48, 5350–5357.

- (28) Schubert, H. L., and Hill, C. P. (2006) Structure of ATP-bound human ATP:cobalamin adenosyltransferase. *Biochemistry* 45, 15188–15196.
- (29) Zoldak, G., Zubrik, A., Musatov, A., Stupak, M., and Sedlak, E. (2004) Irreversible thermal denaturation of glucose oxidase from *Aspergillus niger* is the transition to the denatured state with residual structure. *J. Biol. Chem.* 279, 47601–47609.
- (30) Padovani, D., Labunska, T., and Banerjee, R. (2006) Energetics of interaction between the G-protein chaperone, MeaB, and B₁₂-dependent methylmalonyl-CoA mutase. *J. Biol. Chem.* 281, 17838–17844.
- (31) Leal, N. A., Olteanu, H., Banerjee, R., and Bobik, T. A. (2004) Human ATP: Cob(I)alamin adenosyltransferase and its interaction with methionine synthase reductase. *J. Biol. Chem.* 279, 47536–47542.
- (32) Saridakis, V., Yakunin, A., Xu, X., Anandakumar, P., Pennycooke, M., Gu, J., Cheung, F., Lew, J. M., Sanishvili, R., Joachimiak, A., Arrow-smith, C. H., Christendat, D., and Edwards, A. M. (2004) The structural basis for methylmalonic aciduria. The crystal structure of archaeal ATP: cobalamin adenosyltransferase. *J. Biol. Chem.* 279, 23646–23653.
- (33) Johnson, C. L., Buszko, M. L., and Bobik, T. A. (2004) Purification and initial characterization of the *Salmonella enterica* PduO ATP:Cob(I)alamin adenosyltransferase. *J. Bacteriol.* 186, 7881–7887.